Effect of pressure and supply configuration on mixing efficiency through Venturi effect for co_2/h_2-ch_4/h_2 mixtures in Power-To-Gas process: CFD analysis

Efecto de la presión y configuración de suministro en la eficiencia de mezclado mediante el efecto Venturi para mezclas CO_2/H_2-CH_4/H_2 en el proceso Power-To-Gas: análisis CFD

Efeito da configuração de pressão e alimentação na eficiência de mistura usando o efeito Venturi para misturas de CO2/H2-CH4/H2 no processo Power-To-Gas: análise CFD

Camilo Echeverri-Uribe[1]
Cristian Camilo Mejía Botero[2]
Jhon Jairo Ditta Granados[3]
Andrés Adolfo Amell Arrieta[4]

Received: September 15th, 2023
Accepted: December 5th, 2023
Available: January 10th, 2024

How to cite this article:
C. Echeverri-Uribe, C.C. Mejía Botero, J.J. Ditta Granados, A.A. Amell Arrieta, "Effect of pressure and supply configuration on mixing efficiency through Venturi effect for co2/h2-ch4/h2 mixtures in Power-To-Gas process: CFD analysis", *Revista Ingeniería Solidaria*, vol. 20, no. 1, 2024.
doi: https://doi.org/10.16925/2357-6014.2024.01.09

Research article. https://doi.org/10.16925/2357-6014.2024.01.09

[1] Grupo de Ciencia y Tecnología del Gas y Uso Racional de la energía, Facultad de Ingeniería, Universidad de Antioquia.
e-mail: camilo.echeverriu@udea.edu.co
ORCID: https://orcid.org/0000-0002-9514-4976
CVLAC: https://scienti.minciencias.gov.co/cvlac/visualizador/generarCurriculoCv.do?cod_rh=0001448286

[2] Grupo de Ciencia y Tecnología del Gas y Uso Racional de la energía, Facultad de Ingeniería, Universidad de Antioquia.
e-mail: cristian.mejiab@udea.edu.co
ORCID: https://orcid.org/0000-0002-9291-0014
CVLAC: https://scienti.minciencias.gov.co/cvlac/visualizador/generarCurriculoCv.do?cod_rh=0000117338

[3] Universidad de La Guajira, Facultad de Ingeniería.
e-mail: jditta@uniguajira.edu.co
ORCID: https://orcid.org/0000-0003-0936-0646
CVLAC: https://scienti.minciencias.gov.co/cvlac/visualizador/generarCurriculoCv.do?cod_rh=0000016486

[4] Grupo de Ciencia y Tecnología del Gas y Uso Racional de la energía, Facultad de Ingeniería, Universidad de Antioquia.
e-mail: andres.amell@udea.edu.co
ORCID: https://orcid.org/0000-0003-4473-4105
CVLAC: https://scienti.minciencias.gov.co/cvlac/visualizador/generarCurriculoCv.do?cod_rh=0000039829

Abstract

Introduction: The present article is one of the outcomes of the project "Desarrollo de un sistema "power to gas" (PTG) en el contexto de las fuentes de energía renovables y convencionales disponible en la Guajira" This project was carried out by the University of Antioquia and the University of La Guajira during the period 2019-2023.

Problem: Efficiency and uniformity in gas mixing for Power-to-Gas applications are influenced by pressure variations and supply configurations.

Objective: To assess the impact of pressure variations and supply configurations on the efficiency of the Venturi mixing process, utilizing indicators such as the Z-factor and the coefficient of variation (CoV).

Methodology: Numerical simulations were conducted for four mixer configurations. For CO_2/H_2 mixtures, pressures of 1 bar (case i) and 4 bars (case ii) were considered; for CH_4/H_2 mixtures, pressures of 3 bars (case i) and 35 bars (case ii) were studied.

Results: As the inlet gas pressure increases, uniformity decreases for both mixtures. Horizontal H_2 feeding improves CO_2/H_2 uniformity, while vertical feeding benefits CH_4/H_2 mixing. The mixer reduces CoV by an average of 80% for CO_2/H_2. For CH_4/H_2 mixtures at 3 bars, there is a 60% reduction, but at 35 bars, coefficients increase by 56%.

Conclusion: Pressure and supply configuration significantly influence the mixing process, underscoring the importance of considering these factors in Power-to-Gas applications.

Originality: The study explores the Venturi mixing process in specific gas mixtures for Power-to-Gas applications.

Limitations: The studied conditions and configurations may not encompass all possible scenarios in Power-to-Gas applications.

Keywords: Ventury Type Gas Mixer, CFD study, Mixing performance, Power-to-gas, Hydrogen.

Resumen

Introducción: El presente artículo es uno de los resultados del proyecto "Desarrollo de un sistema "power to gas" (PTG) en el contexto de las fuentes de energía renovables y convencionales disponible en la Guajira" este fue desarrollado por La Universidad de Antioquia y la universidad de La Guajira durante el 2019-2023.

Problema: La eficiencia y uniformidad de la mezcla de gases en aplicaciones Power-to-Gas se ven afectadas por variaciones de presión y configuraciones de suministro.

Objetivo: Evaluar la influencia de variaciones de presión y configuraciones de suministro en la eficiencia del proceso de mezcla Venturi, utilizando indicadores como el Z-factor y el coeficiente de variación (CoV).

Metodología: Se emplearon simulaciones numéricas para cuatro configuraciones de mezcladores. Para mezclas CO_2/H_2, se trabajó a 1 bar (caso i) y 4 bar (caso ii); para mezclas CH_4/H_2, a 3 bar (caso i) y 35 bar (caso ii).

Resultados: A medida que la presión del gas de entrada aumenta, la uniformidad disminuye para ambas mezclas. La introducción horizontal de H_2 mejora la uniformidad de CO_2/H_2, mientras que la alimentación vertical beneficia la mezcla CH_4/H_2. El mezclador reduce el CoV un 80% en promedio para CO_2/H_2. En mezclas CH_4/H_2 a 3 bares, hay reducciones del 60%; a 35 bares aumentan un 56%.

Conclusión: Presión y configuración de suministro influyen en el proceso de mezclado, destacando la importancia de considerar estos factores en aplicaciones Power-to-Gas.

Originalidad: Se explora el proceso de mezclado Venturi en mezclas específicas de gases para aplicaciones Power-to-Gas.

Limitaciones: las condiciones y configuraciones estudiadas pueden no cubrir todos los escenarios posibles en aplicaciones Power-to-Gas.

Palabras clave: Mezclador de Gas Tipo Venturi, Estudio CFD, Rendimiento de Mezcla, Power-to-Gas, Hidrógeno.

Resumo

Introdução: Este artigo é um dos resultados do projeto "Desenvolvimento de um sistema "power to gas" (PTG) no contexto das fontes de energia renováveis e convencionais disponíveis em La Guajira", desenvolvido pela Universidade de Antioquia e pela Universidade de La Guajira durante 2019-2023.

Problema: A eficiência e a uniformidade da mistura de gases em aplicações Power-to-Gas são afetadas pelas variações de pressão e configurações de fornecimento.

Objetivo: Avaliar a influência das variações de pressão e configurações de alimentação na eficiência do processo de mistura Venturi, utilizando indicadores como o fator Z e o coeficiente de variação (CoV).

Metodologia: Foram utilizadas simulações numéricas para quatro configurações de misturadores. Para misturas CO2/H2 trabalhamos em 1 bar (caso i) e 4 bar (caso ii); para misturas CH4/H2, a 3 bar (caso i) e 35 bar (caso ii).

Resultados: À medida que a pressão do gás de entrada aumenta, a uniformidade diminui para ambas as misturas. A introdução horizontal de H2 melhora a uniformidade de CO2/H2, enquanto a alimentação vertical beneficia a mistura de CH4/H2. O misturador reduz o CoV em 80% em média para CO2/H2. Nas misturas CH4/H2 a 3 bars, há reduções de 60%; às 35 barras aumentam 56%.

Conclusão: A configuração da pressão e da alimentação influencia o processo de mistura, destacando a importância de considerar esses fatores nas aplicações Power-to-Gas.

Originalidade: O processo de mistura Venturi é explorado em misturas de gases específicas para aplicações Power-to-Gas.

Limitações: as condições e configurações estudadas podem não abranger todos os cenários possíveis em aplicações Power-to-Gas.

Palavras-chave: Misturador de Gás Tipo Venturi, Estudo CFD, Desempenho de Mistura, Power-to-Gas, Hidrogênio.

1. INTRODUCTION

Renewable energy sources have undeniably become a focal point in the global energy transition, offering a cleaner and more sustainable alternative to conventional fossil fuels[1], [2]. However, one of the foremost challenges hindering the widespread adoption of renewables is their inherent intermittency in energy production[3]. As the sun sets and the winds fluctuate, energy generation from sources such as solar panels and wind turbines experiences inevitable dips and surges [4]. This unpredictability poses a significant hurdle for creating a stable and reliable energy grid.

In response to this challenge, innovative solutions have emerged, and among them, the power-to-gas process stands out as a particularly promising avenue [5]. This technology transforms surplus electricity, often derived from renewable sources like wind or solar power, into gases such as hydrogen or methane. The main goal is to capture and utilize surplus energy that would otherwise go to waste, especially during periods of increased renewable energy production [6].

The Fig. 1 presents a comparison of volumetric storage capacity among various electric energy technologies, with power-to-gas technology (hydrogen and methane storage) demonstrating the highest specific energy storage capacity.

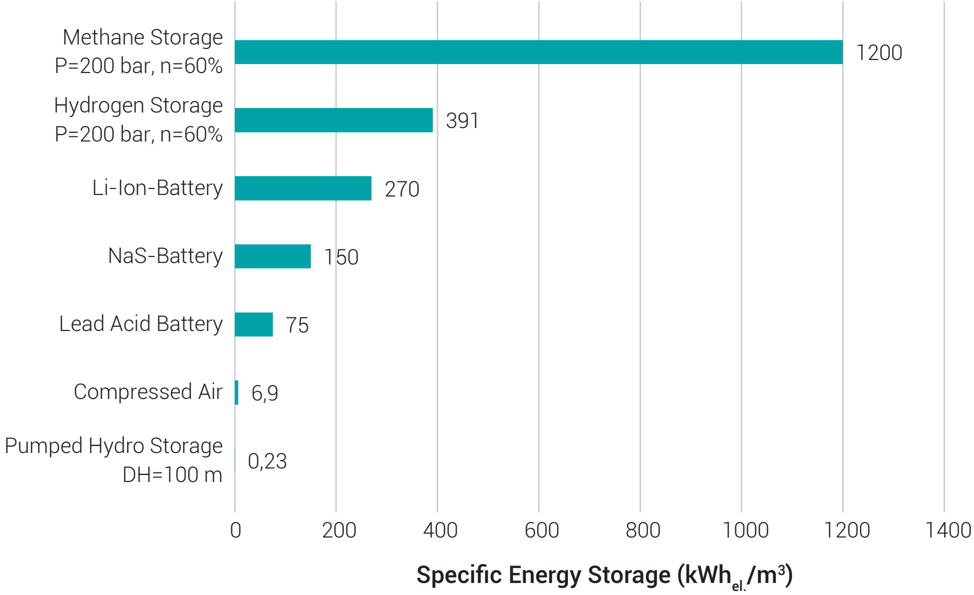

Fig. 1. Volumetric storage capacity across various technologies for electric energy.
Source: Adapted from [7].

This innovative process holds the potential to revolutionize the way we store and utilize renewable energy at a large scale [8]-[10]. The "*Power to Gas with Methanation*" scheme is an innovative approach that integrates renewable energy technologies and energy storage by producing synthetic gas, specifically methane (CH_4), from renewable electrical sources like solar or wind energy (see Fig. 2). This process aims to harness surplus renewable energy during periods of low demand and convert it into a versatile energy carrier, such as methane, which can be stored and utilized across various applications [11]. The scheme consists of several stages. Initially, excess electric energy from renewable sources is captured and used to perform water electrolysis in an electrolyzer, noteworthy is the fact that electrolysis is considered one of the most promising technologies for hydrogen production [12], [13] due to its capability to utilize inherently intermittent renewable electricity sources [14], such as solar and wind energy as shown in Fig. 2. This process splits water into its fundamental components, hydrogen (H_2), and oxygen (O_2). The produced hydrogen is stored and employed in the methanation stage or in a blending with CH_4 for use in a combustion system.

The methanation stage involves combining the produced hydrogen with carbon dioxide (CO_2), which can be captured from industrial sources or directly from the air, through the Sabatier reaction ($4H_2+CO_2 \rightarrow CH_4+2H_2O$). The generated methane gas, also known as synthetic gas or biomethane, can be stored and used in diverse applications such as electricity and heat generation, feeding existing natural gas networks, or even serving as fuel for transportation vehicles [11] [15]. Additionally, it offers the opportunity to utilize existing gas infrastructure and harness methane as a long-term energy storage method [16].

Fig. 2 illustrates, with a dash-point, the placement of mixers in the power-to-gas scheme. The incorporation of a mixing system is important to attain a consistent uniformity of gas concentrations, mitigating issues in the conversion efficiency of the methanation process or preventing instabilities in combustion systems.

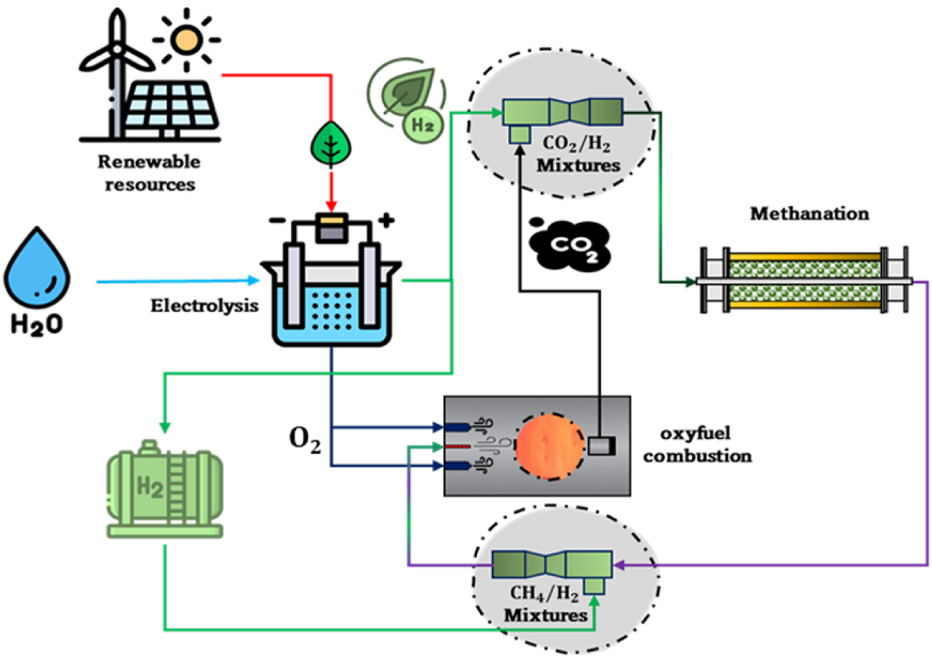

Fig. 2. The schematic depiction of the "Power-to-Gas" process.
Source: own work**.** Except for the oxy-combustion furnace, mixers, and the Methanation Reactor, all icons have been obtained from Flaticon.com.

Within the context of energy transition and decarbonization, a viable alternative is the implementation of H_2/CH_4 blending. This approach aims to mitigate CO_2 emissions by substituting a portion of CH_4 with H_2, where the combustion of the latter produces water as a byproduct.

This paper is dedicated to a numerical analysis of the mixing process involving two essential gas mixtures: CO_2/H_2 and CH_4/H_2. The examination of the first mixture is essential as these gases are employed in the production of synthetic methane through a methanation process. The second case (CH_4/H_2) is investigated due to its relevance as a mixture within a gas network blending scenario, particularly in an in-situ application. Central to this analysis is a mixer that capitalizes on the Venturi effect for its operation. The fundamental objective is to meticulously evaluate the influence of pressure variations and distinct supply configurations on the efficiency of the mixing process and the uniformity of gas concentrations.

An important aspect of the blending process involves ensuring efficient mixing to achieve a uniform composition of gases. This is particularly important in combustion systems where the presence of a stratified gas composition may lead to stability challenges (flashback or lift-off). This is where the Venturi effect, a phenomenon rooted in fluid dynamics, enters the scene [17]-[22]. The principle behind the Venturi effect is ingeniously simple: when a fluid flows through a narrow section of a conduit, the constriction triggers a reduction in pressure, causing the fluid to accelerate. This acceleration, in turn, fosters more thorough mixing of different components within the flow. Therefore, our focus is on analyzing the Venturi effect as an efficient solution for gas mixing, given its ease of construction in contrast to other mixers, like static mixers, which often feature complex geometries. Haddadi et al. [23] evaluated four configurations of a static mixer by using CFD and comparing the Z-factor and coefficient of variation (CoV) to determine which one presents the best performance. Fourcade et al. [24] evaluated a method, using CFD, to calculate the average value of the rate of striation thinning in order to determine the mixing quality.

The analysis was carried out based on metrics such as the coefficient of variation and the Z-factor, which serve as critical indicators of concentration uniformity and mixing efficiency. These metrics provide deeper insights into the intricacies of the mixing process and shed light on the interplay between various parameters.

As the analysis progresses, the paper ventures into the realm of insights and conclusions. Here, the impact of pressure fluctuations and different supply configurations on the overall performance of the mixing process takes center stage. The paper underscores the significance of these factors and offers practical recommendations for achieving an optimal distribution of gases. Understanding the impact of pressure variations and diverse supply configurations on mixing efficiency and gas concentration uniformity is important for optimizing system performance.

2. MATERIALS AND METHODS

2.1. Geometry, Flow Configurations, and Operating Conditions

The geometry employed for the mixing of CO_2/H_2 and CH_4/H_2 flows is based on the Venturi effect, a type of device extensively utilized in the state of the art for mixing various types of fluids [20]-[22]. This device falls under the category of a static mixer, distinguished by its lack of moving components within and regarded as equipment of relatively straightforward construction and operation. Gas feed is facilitated through an arrangement of tubes in a "T" shape. The inner diameter of the inlet conduits for the compounds measures 2.6645 cm, equivalent to a commercial 3/4" sch.40 pipe. The neck diameter of the Venturi is 1.5 cm, while the exit diameter of the mixer is 3.5053 cm, corresponding to a commercial 1" sch.40 pipe. Fig. 3 illustrates a schematic representation of the geometry used and the corresponding mesh. In section 2.4 details about the mesh are provided.

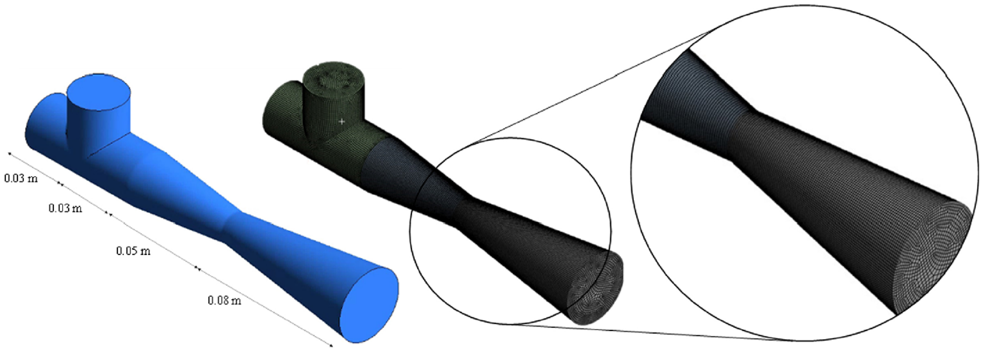

Fig. 3. Mixer's geometry and corresponding mesh.
Source: own work.

In this study, the impact of inlet flow configurations and pressure on mixing performance is investigated for CO_2/H_2 and CH_4/H_2 mixtures. The introduction of flows plays an important role, as it can impact the efficiency of the mixing process. The objective is to determine which of these configurations proves most favorable in terms of achieving a homogeneous gas distribution and maximizing interaction. It is noteworthy that the gases under investigation exhibit distinct physical and transport properties, such as density and diffusivity. Consequently, the method of introducing gases into the mixer is expected to be crucial for performance, given these differences.

The second variable under examination is pressure. It is of interest to understand its effect on flow mixing. The CO_2/H_2 mixture in a relation of 1/4 is employed in the methanation reaction according to the Sabatier reaction, a volume-consuming process. Le Chatelier's principle suggests that increasing pressure within the reactor enhances conversion rates [25]. Additionally, the chemical kinetics of methanation also favor the application of higher pressure, as substantiated and confirmed in [26]. Consequently, CO_2/H_2 mixing is studied under pressures of 1 bar and 4 bar, and both gases must be supplied to the reactor at the same pressure based on experimental experiences [26]. When the pressure of one gas is higher than that of another, it induces the hydraulic buffer effect, preventing the gas with lower pressure from flowing through the pipe.

In the case of CH_4/H_2 mixtures, they are intended for use as fuel in an oxy-combustor integrated into the PtG system, as illustrated in Fig 1. The fuel mixture is composed of 15% H_2 and 85% CH_4 by volume, according to the maximum allowed in the state of the art [27]. The utilization of volumetric percentages of these mixtures is grounded in studies [28], [29], which indicate that implementing H_2 at low concentrations (below 15% by volume) could permit its introduction into gas pipelines without significant increase in associated risks (countries analyzed in [28], [29] mostly correspond to European Union nations).

The examined pressures are 3 bar and 35 bar and the flow rate is 1 Sm^3/h. The choice of 3 bar is informed by the fact that burners typically operate at pressures above atmospheric to account for pressure drops in their supply lines. On the other hand, the selection of the flow rate and the pressure of 35 bar is based on the maximum pressure supplied by an AEM electrolyzer manufactured by ENAPTER [30] and the flow rate produced by two electrolyzers of 0.5 Sm^3/h each which corresponds to a mass flow rate of 0.085 kg/h. The aim is to ensure proper mixing of mentioned reactants before they are directed to the burner. For clarity, a summary of the inlet configurations and operating conditions is presented in Table 1. The gas temperature was 300 K as gases lose heat through piping until they reach the mixer and cool to atmospheric temperature.

Table 1. Flow configurations and inlet operating conditions

Mixtures	Inlet Configuration	Pressure [bar]	H_2 Flow [Sm^3/s]	CO_2 Flow [Sm^3/s]	CH_4 Flow [Sm^3/s]
H_2/CO_2	Vertical H_2/ Horizontal CO_2	1	2.778E-04	6.944E-05	----
		4	2.778E-04	6.944E-05	----
	Horizontal H_2/ Vertical CO_2	1	2.778E-04	6.944E-05	----
		4	2.778E-04	6.944E-05	----
H_2/CH_4	Vertical H_2/ Horizontal CH_4	3	1.742E-04	----	9.872E-04
		35	1.742E-04	----	9.872E-04
	Horizontal H_2/ Vertical CH_4	3	1.742E-04	----	9.872E-04
		35	1.742E-04	----	9.872E-04

Note: For all conditions, a temperature of 300 K was used.

Source: own work.

2.2. Governing Equations

The fundamental equations utilized in the numerical simulation are presented hereafter. Any fluid flow problem necessitates, at minimum, the solution of the Navier-Stokes (NS) equations, which encompass the equations of mass conservation (continuity equation) and conservation of linear momentum (equation (1)); these govern fluid motion. For this analysis, flows through the mixer are considered non-isothermal and multicomponent, thus necessitating the inclusion of the energy conservation equation and species conservation equation (equations (2) and (3)) [31]. The latter two were solved using the full multicomponent diffusion option due to the working fluid being H_2, characterized by a high molecular diffusivity. Additionally, the standard k-ε turbulence model with standard wall function was employed to resolve turbulence within the system, since this model has been validated in other mixing system studies [32], [33].

$$\frac{\partial \rho}{\partial t} + \nabla.(\rho \boldsymbol{u}) = 0$$

$$\frac{\partial(\rho \boldsymbol{u})}{\partial t} + \nabla(\rho \boldsymbol{u}\boldsymbol{u}) = -\nabla \mathrm{p} + \nabla.\boldsymbol{\tau} + F \tag{1}$$

$$\frac{\partial(\rho E)}{\partial t} + \nabla.\big((\rho E + p)\boldsymbol{u}\big) = \nabla.\left(\mathrm{k}\nabla T - \sum_j h_j \boldsymbol{J}_j + (\boldsymbol{\tau}.\boldsymbol{u})\right)$$

$$E = U + \frac{u^2}{2} + \Phi \tag{2}$$

$$\frac{\partial(\rho Y_i)}{\partial t} + \nabla.(\rho Y_i \boldsymbol{u}) = -\nabla.\boldsymbol{J_i}$$

$$\boldsymbol{J}_j = -\rho D_{i,m} \nabla Y_i - D_{i,T} \nabla T/T \tag{3}$$

Where $\boldsymbol{u}$ is the fluid velocity vector (SI unit: m/s), ρ is the fluid density (SI unit: kg/m³), p is the fluid pressure (SI unit: Pa), F is the volumetric force vector (SI unit: N/m³), τ is the viscous stress tensor (SI unit: Pa). The considered forms of the Navier-Stokes equations are applicable in single-phase flows. It is crucial to emphasize their validity is confined to Newtonian fluids, where the viscous stress tensor simplifies to being proportional to the rate of strain tensor $-\tau=2\mu S$, with μ as the dynamic viscosity of the fluid (SI unit: Pa.s) and $S=(1/2)(\nabla u+(\nabla u)^T)$. For the energy equation, E represents the total system energy per unit mass (SI unit: J/kg), decomposed into different contributions, including internal energy (U), kinetic energy ($u^2 / 2$), and potential energy (Φ), all expressed per unit mass. On the other hand, the variable T represents the temperature field (SI unit: K), while Y_i represents the molar fraction field of a particular species. The diffusive flux of species molar fraction is denoted as J_j and is assumed to follow Fick's law. This implies that the flux can be broken down into two components: one related to molecular diffusion due to a concentration gradient and another related to thermal diffusion, as a consequence of the temperature gradient. $D_{i,m}$ and $D_{i,T}$ are respectively the mass and thermal diffusivity of the i-th species (SI unit: m^2/s).

2.3. Numerical Method

For the simulations in this study, the computational fluid dynamics (CFD) software ANSYS Fluent 19.2 [34] is employed. This software employs an Eulerian approach to solve the Reynolds Averaged Naiver Stokes (RANS) equations using a cell-centered finite volume discretization. Both the ideal gas mixing law and multicomponent diffusion were implemented due to the presence of hydrogen, which exhibits high molecular diffusion. The flow and scalar equations are solved sequentially in double-precision format. The spatial discretization of the linear momentum and mass transfer equations is accomplished using a second-order scheme. Diffusion terms are approximated using a central difference scheme, ensuring second-order accuracy. To couple the pressure and velocity fields, the SIMPLE algorithm proposed by [35] is utilized. The selection of these schemes and formats is based on the positive outcomes observed in the study conducted by [36].

2.4. Meshing

Meshing, or domain discretization, is a pivotal step in computational fluid dynamics (CFD) simulations [37]. In this work, to attain an optimal mesh, three entirely structured meshes of 125,000 (M1), 328,000 (M2), and 500,000 (M3) elements were generated to the Vertical H_2/Horizontal CO_2 configuration and a pressure of 4 bar. The equi-angle skewness and aspect ratio were both below 0.24 and 4, respectively. Fig. 4 shows the results obtained for (a) velocity and (b) the CO_2 molar fraction along the central line of the mixer. As observed, the CO_2 molar fraction exhibited the same behavior along the mixer for all three mesh configurations. However, after the expansion process in the Venturi (x=0.11 m), a slight discrepancy is noted in the results obtained with the M1 mesh. Therefore, the simulations were carried out using the 328,000-element mesh (M2), as from this point, significant changes in the system response were not generated. It is worth mentioning that this procedure was replicated for the H_2/CH_4 mixtures, yielding analogous outcomes. Consequently, the M2 mesh was also selected for simulations involving these mixtures.

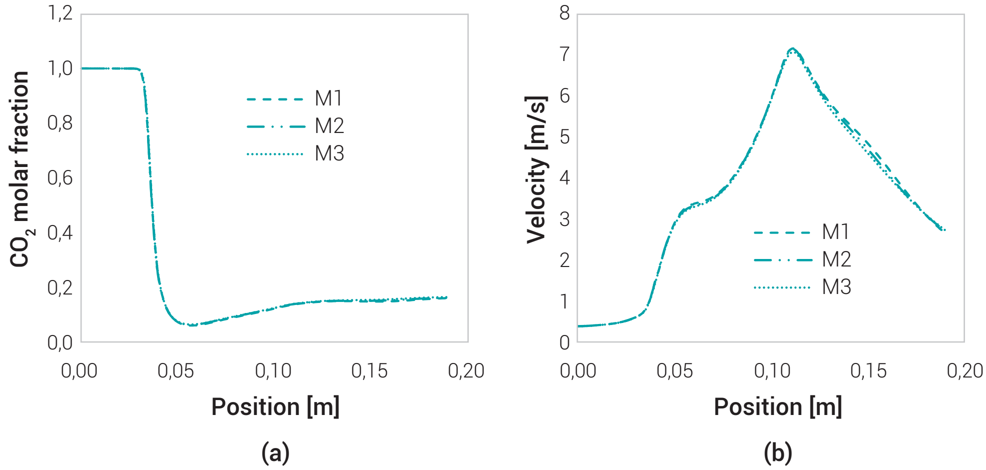

Fig. 4. Mesh independence with results of (a) CO_2 molar fraction and (b) velocity.
Source: own work.

2.5. Evaluation of the Mixer

To assess the achieved efficiency in the mixing process, it is essential to acquaint oneself with the criteria employed for this purpose. However, before delving into these criteria, it is pertinent to highlight the two widely referenced types of mixing in scientific literature: distributive mixing and diffusive mixing [38].

In *distributive mixing*, relatively large eddies exchange positions and convect the material in such a way that at an observation scale greater than the eddy size, a macroscopic concentration uniformity emerges. At a scale much smaller than the eddy size, significant mixing does not occur. In *dispersive mixing*, the larger eddies from distributive mixing reduce in size through the turbulent shear effect, resulting in a finer-grained mixture. On a molecular scale, mixing remains highly segregated. Fig. 5 illustrates the distinction between these two types of mixing, but it is important to note that both are always present in mixing.

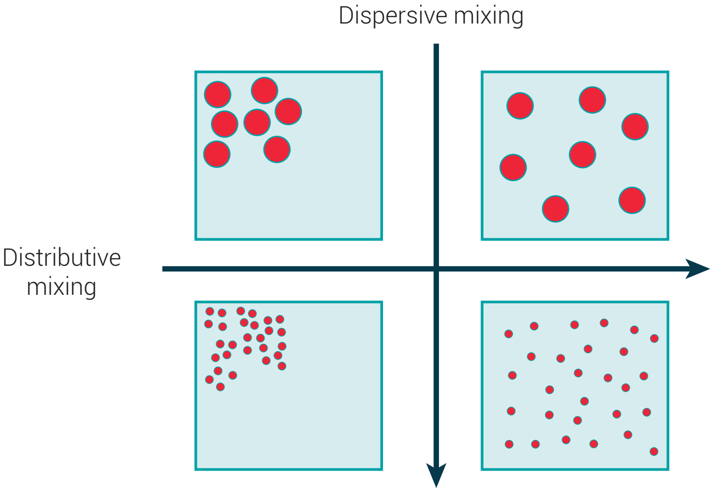

Fig. 5. Distributive and dispersive mixing.
Source: Adapted from [39], [40].

Considering the above, the most common parameters for evaluating mixing systems are the Z-factor and the Coefficient of Variation (CoV) [23]. The former accounts for the pressure drop during mixing and is defined as the ratio of pressure drop in the static mixer, ΔP, to the pressure drop in an empty pipe (without the mixer), ΔP_0, as presented in equation (4). ΔP_0 is obtained from a simulation of a straight tube without convergent/divergent sections, and utilizing the same numerical setup.

$$Z = \frac{\Delta P}{\Delta P_0} \tag{4}$$

On the other hand, the CoV corresponds to the standard deviation of the mass concentration of a compound in the mixture, serving as a measure of the uniformity achieved during the mixing process. For the calculation of this coefficient, equation (5) is employed, where Y_i represents the local mass fraction at the i-th point, N is the number of evaluation points, and Y_{mean} is the average mass fraction in the cross-sectional area of the pipe.

$$CoV = \sqrt{\frac{\sum_{i=1}^{N}(Y_i - Y_{mean})^2}{N-1}}\frac{1}{Y_{mean}} \tag{5}$$

As evident from equations (4) and (5), performance parameters necessitate evaluating the system in the absence of the mixer to ascertain effects genuinely caused by the equipment itself rather than the diffusive and viscous behavior inherent to gases. For this reason, simulations must be performed with the system devoid of the Venturi tube, as depicted in Fig. 6, to thus assess how much the coefficient of variation of concentration improves when the mixer is employed and to determine the associated pressure drop. In this case, the equi-angle skewness and aspect ratio were both below 0.44 and 9, respectively.

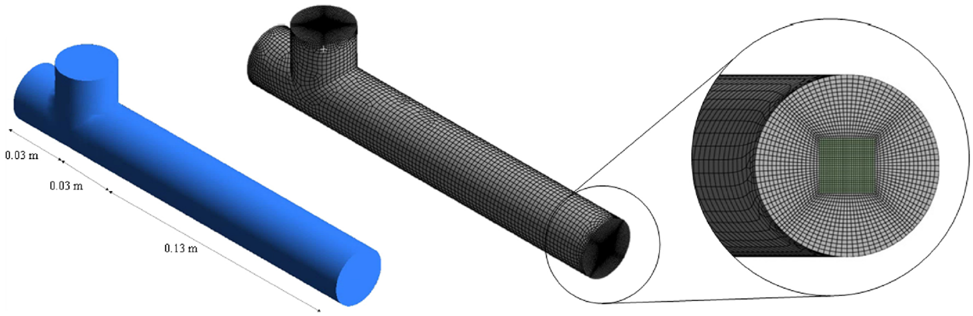

Fig. 6. Geometry without mixer and corresponding mesh.
Source: own work.

The lower the CoV, the more uniform the mixing, and the closer the Z-factor is to one, the lower the pressure drop of the mixer.

3. RESULTS

3.1. H_2/CO_2 Mixing

Fig. 7 displays the mass fraction contours of CO_2 for the four evaluated configurations in (a) mixer operation and (b) non-mixer operation. It is evident that an increase in pressure leads to a decrease in concentration uniformity across all evaluated configurations. Similarly, adding hydrogen horizontally yields an enhancement in contour uniformity. When hydrogen is introduced from a vertical position, its penetration into the tube is constrained by its lower density, leading it to predominantly flow along the upper wall of the pipe. Moreover, a notable improvement in mixing is observed when comparing Fig. 7 (a) to Fig. 7 (b), indicating that the Venturi's use exerts a significant effect on mixing, and the achieved uniformity is not solely attributed to the diffusive effects of gases. Fig. 8 illustrates the CoV for all evaluated configurations with and without the mixer. It is evident that an average decrease of approximately 80% in the CoV is observed when comparing configurations without the mixer to configurations with the mixer. This substantial increase in concentration uniformity is demonstrated by utilizing the mixer. Additionally, it can be noted that the most critical condition in terms of uniformity occurs for the vertical H_2 feed at 5-bar pressure, which exhibits a CoV of 16.22%. However, this effect is compensated for when the H_2 is fed horizontally, resulting in a CoV of 9.09%, which is comparable to the values obtained for the 1-bar pressure conditions. This is due to the higher turbulence along the mixer when H_2 is fed horizontally since it has a higher volumetric flow.

Nevertheless, none of the studied options ensures homogeneous mixing, necessitating the consideration of alternative mixer configurations, such as static mixers. While these may generate higher pressure drops due to mixing elements, they offer the potential for improved mixing quality.

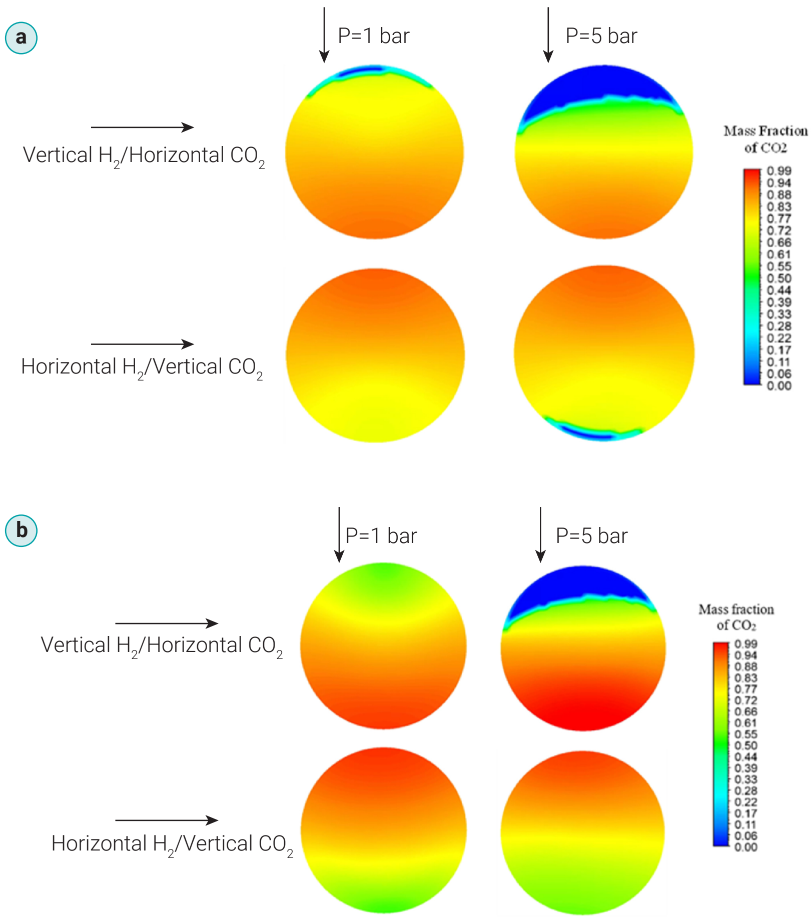

Fig. 7. CO_2 concentration contours at mixer outlet for (a) with mixer and (b) without mixer.
Source: own work.

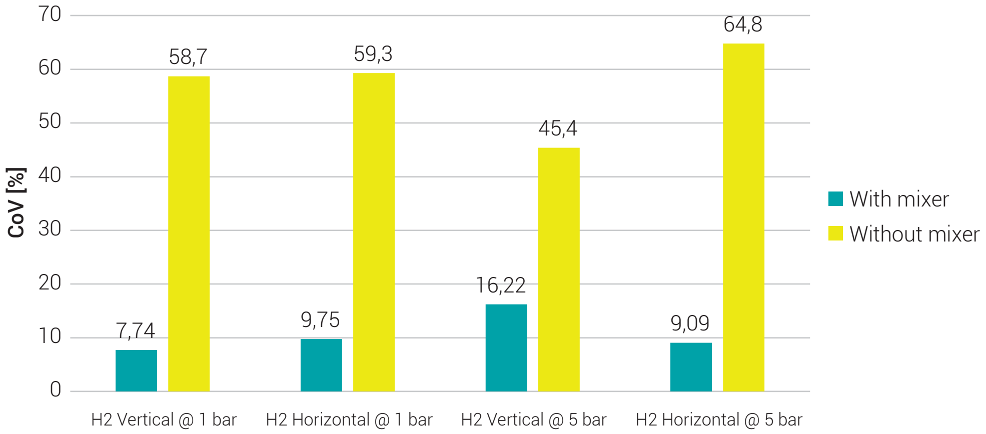

Fig. 8. Coefficient of Variation for H_2/CO_2 mixture case.
Source: own work.

To comprehend the previous behavior, Fig. 9 illustrates the velocity profile for all evaluated configurations within the mixer. As discernible, there is an increase in velocity across all configurations as it approaches the intersection zone of the two streams in the T-shaped pipe (x=0.03 m), attributed to the augmented volumetric flow resulting from the combined streams. Additionally, a rise in mixture velocity is observed from the entry to the Venturi tube (x=0.06 m) up to x=0.11 m due to the reduction in the cross-sectional area of the tube. Beyond this point, velocity decreases due to the enlargement of the cross-sectional area, which aligns with the expected Venturi effect.

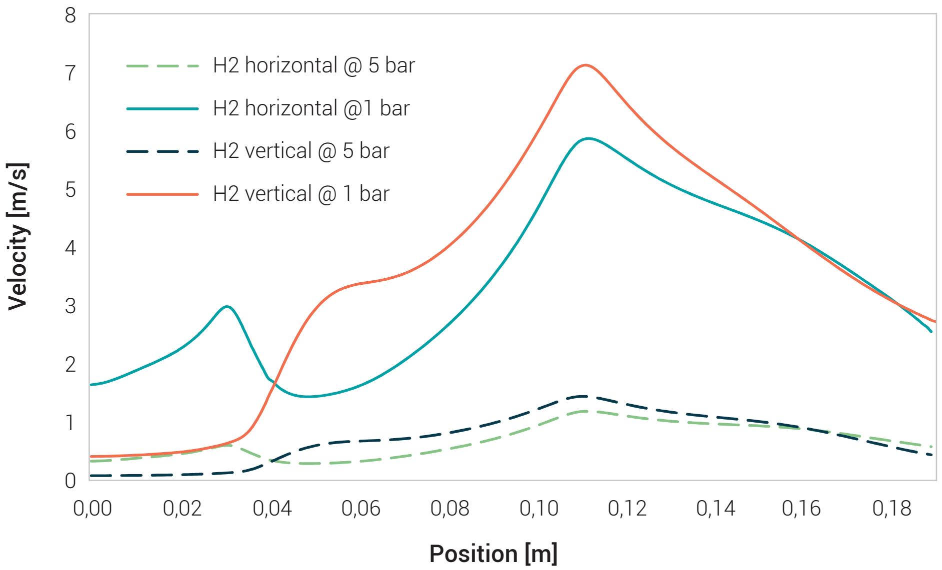

Fig. 9. Velocity profile along the mixer for the evaluated configurations.
Source: own work.

It's important to note that, regardless of the evaluated configuration, at the operating conditions of 5 bar, a lower velocity is observed along the mixer. This underscores that low pressures lead to a more turbulent condition within the equipment, significantly enhancing mixing, as depicted in Fig. 7. Moreover, according to kinetic theory, at higher pressures mass diffusivity decreases which is in line with the results. However, this effect can be compensated for by feeding H_2 through the horizontal tube. As this compound is fed at a higher volumetric proportion, turbulence is increased at the intersection zone in the T-shaped pipe. This is evident in Fig. 9, where a higher velocity is present in the intersection zone for both pressures when H_2 is fed through the horizontal configuration.

Fig. 10 (a) and (b) illustrate the pressure profile along the mixer for the 1 and 5 bar configurations, respectively. As observed, the data is presented in pascals to enhance visualization, given that pressure drop was nearly insignificant for all evaluated configurations. Moreover, the effect of adding H_2 vertically or horizontally does not significantly alter the pressure drop. Additionally, the pressure profile for the evaluated configurations without a mixer is presented, allowing direct observation of the mixer's effect on this parameter, isolating the viscous effects inherent to the gas mixture. It is noticeable that, in the configuration with a mixer, a pressure drop occurs as it approaches the neck of the Venturi (x= 0.11 m), consistent with Bernoulli's law, which states that increasing velocity reduces the stream's pressure to conserve system energy. This effect is countered after the Venturi neck due to the increased cross-sectional area of the mixer, resulting in reduced velocity and increased pressure. As the gas approach the converging section of the mixer, their pressure increases as a consequence of the increase in velocity (Venturi effect). In this way, it is guaranteed that energy is conserved within the system. Subsequently, the gases enter the divergent section, decreasing the speed again and increasing the pressure. However, the final pressure is slightly less than the initial one, observing slight pressure drops that do not seem to be highly influenced by the initial pressure of the gases. The final pressure drop corresponds to the difference in pressures between the inlet and outlet of the mixer, yielding values of 4.8 Pa (4.8e-5 bar) and 1.02 Pa (1.02e-5 bar) for the 1 and 5 bar configurations, respectively. This illustrates the low pressure drop inherent to these devices.

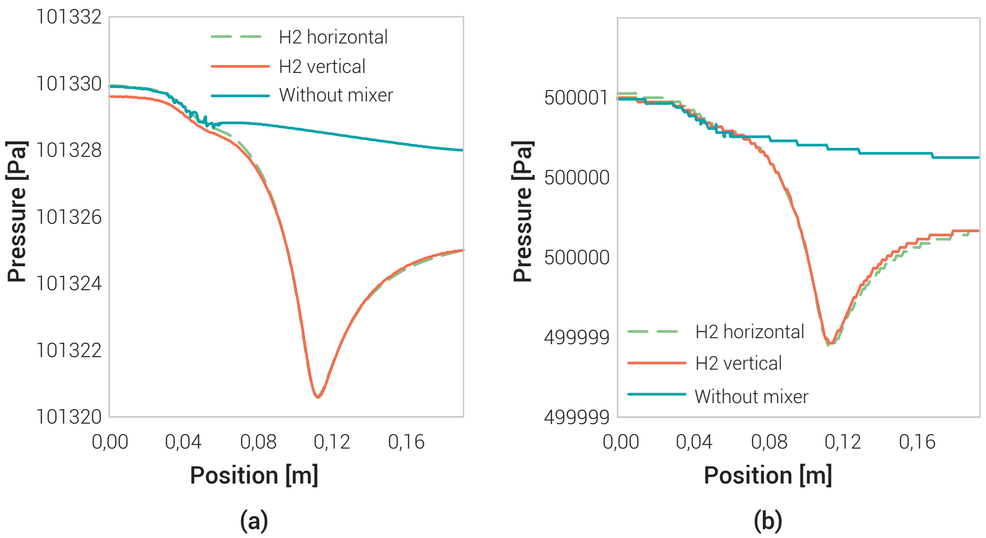

Fig. 10. Pressure profile in the mixer for (a) 1 bar operating condition and (b) 5 bar operating condition.
Source: own work.

To relate the pressure drop between the system with and without the mixer, the use of the factor Z, as shown in equation (4), is employed. This equation also presents the coefficient of variation (CoV), which serves as a criterion for concentration uniformity at the mixer outlet.

Fig. 11 depicts the factor Z for all evaluated conditions. It is evident that values close to two are presented for all configurations, indicating that the pressure drop generated by the system with the mixer corresponds to approximately twice the pressure drop generated in the absence of the mixer. Nevertheless, as observed in Fig. 10, the pressure drops generated are insignificant, indicating that this type of mixer is suitable in terms of energy performance and its use does not significantly affect the pressure required for the methanation reactor.

Thus, considering that high pressures are a requirement for the methanation reactor, the suitable configuration according to the conducted analysis is through the horizontal feed of H_2. This configuration yields acceptable uniformity with negligible pressure drop.

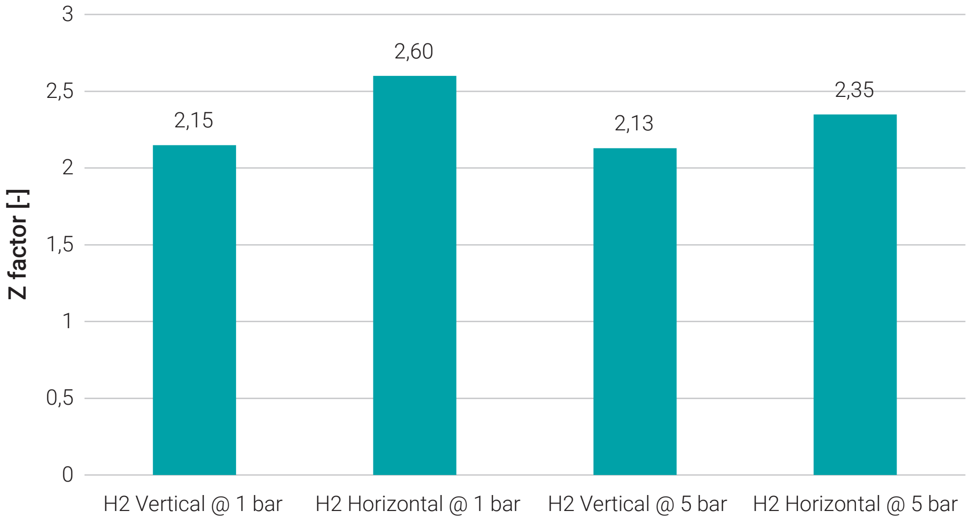

Fig. 11. Coefficient of Variation and (b) Factor Z for the Evaluated Conditions.
Source: own work.

Finally, an important factor in flow systems is the roughness of the tube. A high rugosity can generate energy losses due to the wall/gas friction, and increase the pressure drop in the system. Nonetheless, for the mixer dimensions considered it is not expected to have a significant effect on their performance. In the present work, a fixed roughness was selected, and the effect of this parameter on the mixing performance is outside the scope.

3.2. H_2/CH_4 Mixing

In Fig. 12, contour plots of the molar fraction for the four evaluated conditions are shown with vertical and horizontal H_2 feed, for (a) with mixer and (b) without mixer. As can be observed, for the 3 bar pressure condition, the greatest uniformity is achieved with the vertical H_2 feed, once again highlighting the advantage of horizontally feeding the fluid requiring a higher volumetric flow, which, in this case, is CH_4. This is due to the greater turbulence observed at the intersection in the T-shaped tube under these conditions. In the case of the 35 bar pressure, optimal mixing is not achieved, as evidenced by the presence of different contour colors for the option with a mixer. Nonetheless, a significant improvement compared to the no-mixer condition is observed. Furthermore, as in the case of 3 bar, the vertical H_2 feed configuration with a mixer yields better results, although it is important to note that the mixing is still not optimal.

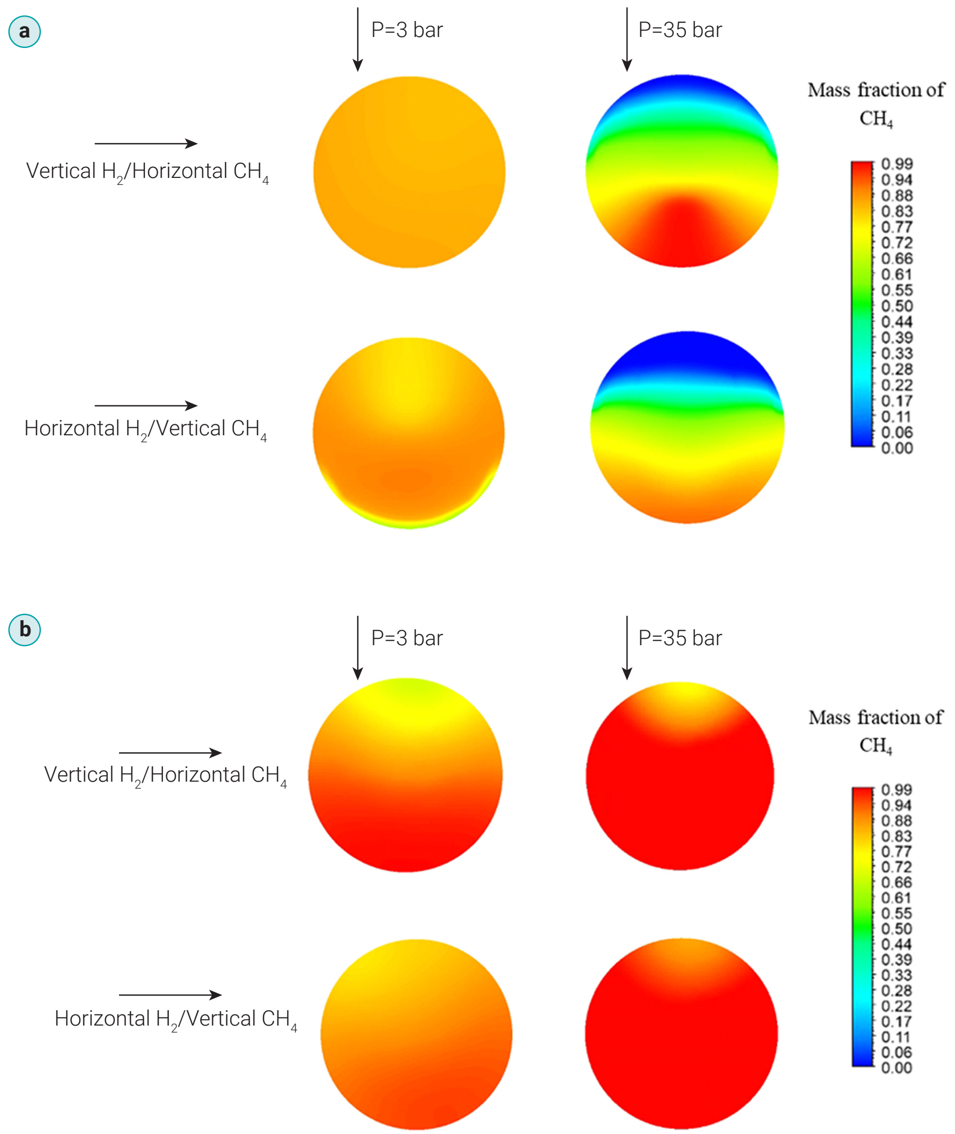

Fig. 12. Contours of methane molar fraction at the mixer outlet for (a) with mixer and (b) without mixer.
Source: own work.

Fig. 13 displays the pressure profile along the mixer for (a) a pressure of 3 bar and (b) a pressure of 35 bar. As observed, analogous to the situation in the CO_2/H_2 mixer, a similar profile is exhibited when adding H_2 vertically and horizontally, with practically negligible pressure drops.

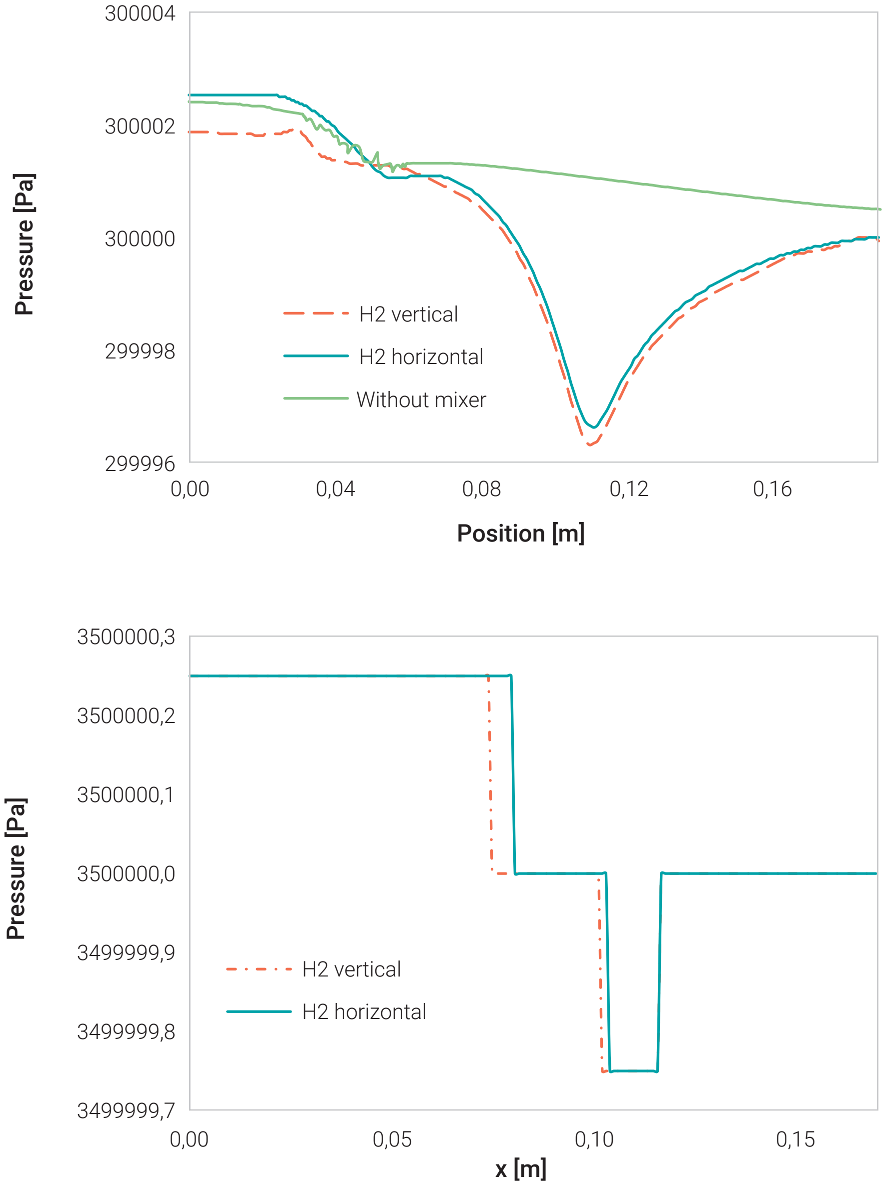

Fig. 13. Pressure profiles for (a) P=3 bar and (b) P=35 bar.
Source: own work.

In Fig. 14 (a), the coefficient of variation is presented for the evaluated conditions. For the pressure of 3 bar, a significant reduction in this parameter is observed (on the order of 60% on average) when using the mixer for both H_2 feeding conditions. This highlights the advantage of using this equipment as it significantly improves concentration uniformity. However, a particularly remarkable improvement is noted when feeding H_2 vertically, confirming the analysis derived from the contours shown in Fig.

12. On the other hand, Fig. 14 (b) depicts the Z factor for the evaluated conditions, revealing that under these circumstances, a pressure drop very similar to that obtained without mixing is observed. Nevertheless, as seen in Fig. 13, the resulting pressure drop is negligible.

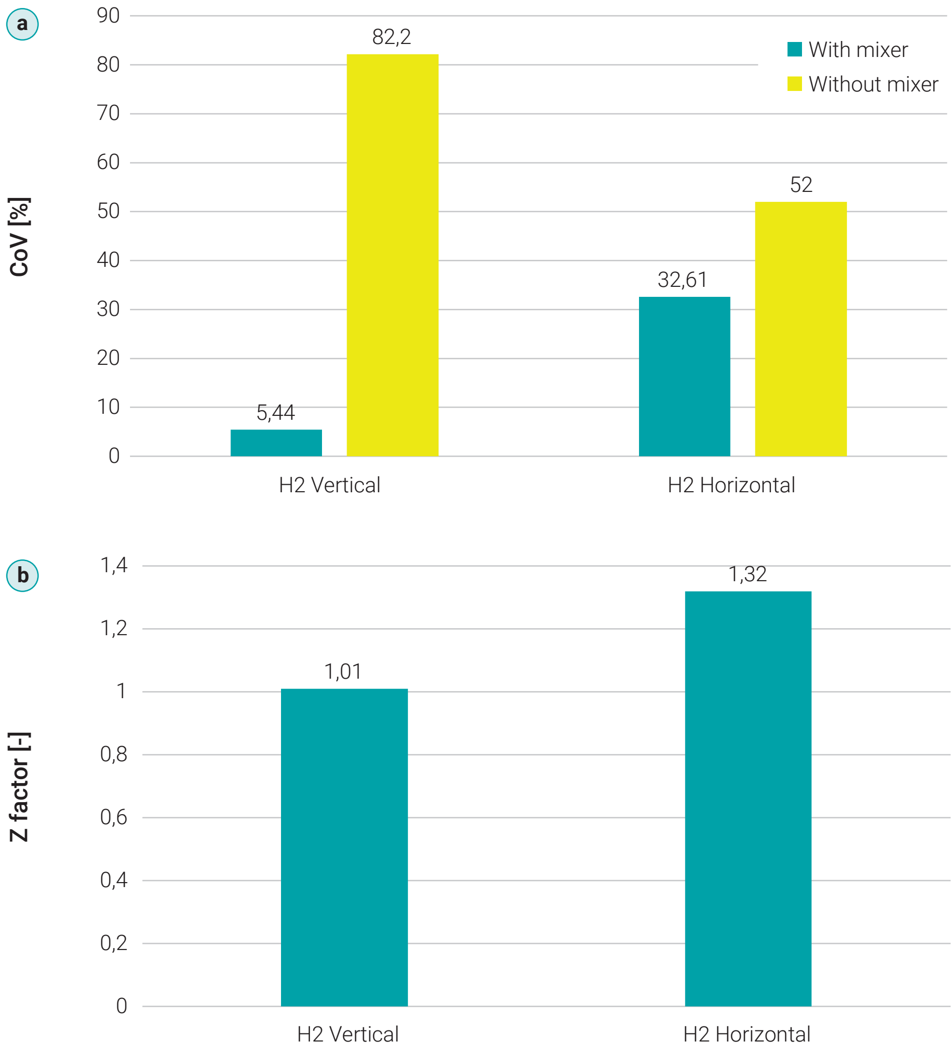

Fig. 14. (a) Coefficient of Variation (CoV) and (b) Z Factor for P=3 bar.
Source: own work.

In Fig. 15, the coefficient of variation and the Z factor are presented for a pressure of 35 bar. As observed in Fig. 15 (a), the coefficients of variation are very high (increasing by an average of 56%), indicating that for pressures around 35 bar, the proposed configuration is not recommended and alternative options, such as a longer configuration or a different design, should be evaluated. It is also noticeable that the coefficients of variation for the configuration without a mixer are lower; however, it should be noted, as mentioned earlier, that in the configuration without a mixer, there are nearly 100% CH_4 molar fractions. On the other hand, in Fig. 15 (b), the Z factor is very close to 1, indicating that the pressure drop is low, consistent with what was previously mentioned in the pressure profile.

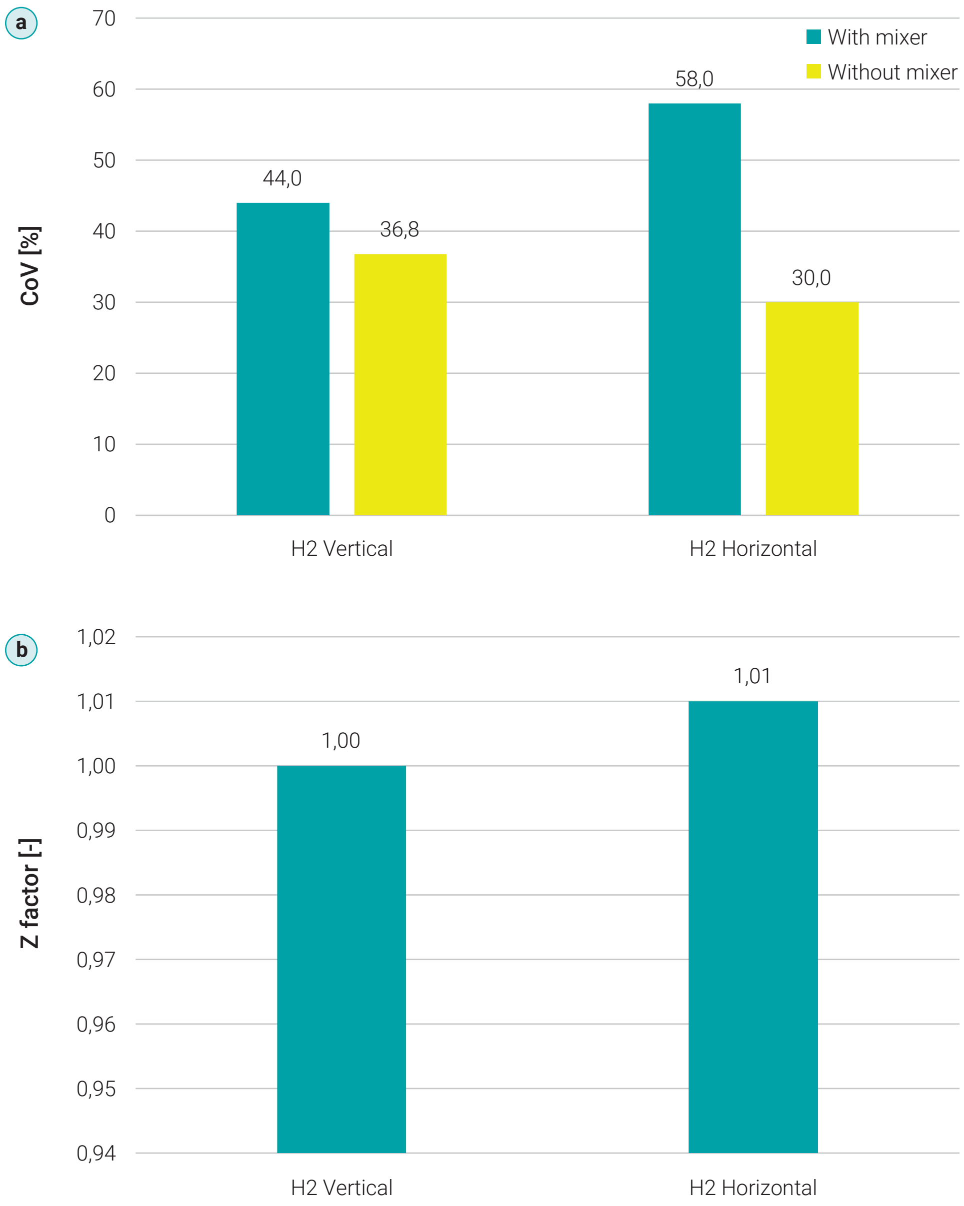

Fig. 15. (a) Coefficient of Variation (CoV) and (b) Z Factor for P=35 bar.
Source: own work.

The aforementioned behavior regarding the decrease in mixing at higher pressures (3 bar compared to 35 bar) can be explained through the theory of transport phenomena, more specifically with the binary diffusion coefficient, which is presented in the following equation [39] [40].

$$D_{i,j} = \frac{1.8583 \times 10^{-7}\left[T^3\left(W_i + W_j\right)/\left(W_i . W_j\right)\right]^{1/2}}{p\sigma_{i,j}^2 \Omega_{i,j}^{(1,1)*}(T*;\ \delta *)} \quad (m^2/s) \tag{6}$$

Where the subscripts i and j refer to the chemical species, p is the pressure (unit: atm), $\sigma_{i,j}$ is the average particle diameter, W is the molecular weight (unit: kg/kmol), and $\Omega_{i,j}^{(1,1)*}(T*;\ \delta *)$ is the collision integral which depends on the reduced temperature of both gases and whether the gases are polar or non-polar. According to the above expression, the binary diffusion coefficient is inversely proportional to the pressure, meaning that at higher pressure, the diffusion coefficient decreases, thus negatively affecting mixing. Additionally, pressure has an effect on convection, as will be discussed in the following section.

Pressure Effect on Velocity

Pressure has an important effect on velocity, since the latter depends on the density and mass flow of the gases. In this case, regardless of the initial pressure, it is desired to leave the mass flow of the reactants constant, so an increase in pressure generates an increase in density and therefore a decrease in velocity. So, the flow at 35 bar has a lower volumetric flow rate compared to the 3 bar condition. This can be seen in Fig. 16, where at 3 bar, the flow velocities reach a maximum of approximately 2.5 m/s, while for 35 bar, the maximum velocity is around 0.2 m/s. This implies that besides the decreased diffusivity coefficient at higher pressures, due to the decreased velocity, the convective mass transfer coefficients also decrease. As a result, there is a combined effect that negatively impacts mixing as the system pressure increases. Finally, it is observed that comparing the horizontal and vertical configurations at each pressure level, the velocity profiles are very similar with only slight differences at the beginning of the mixer.

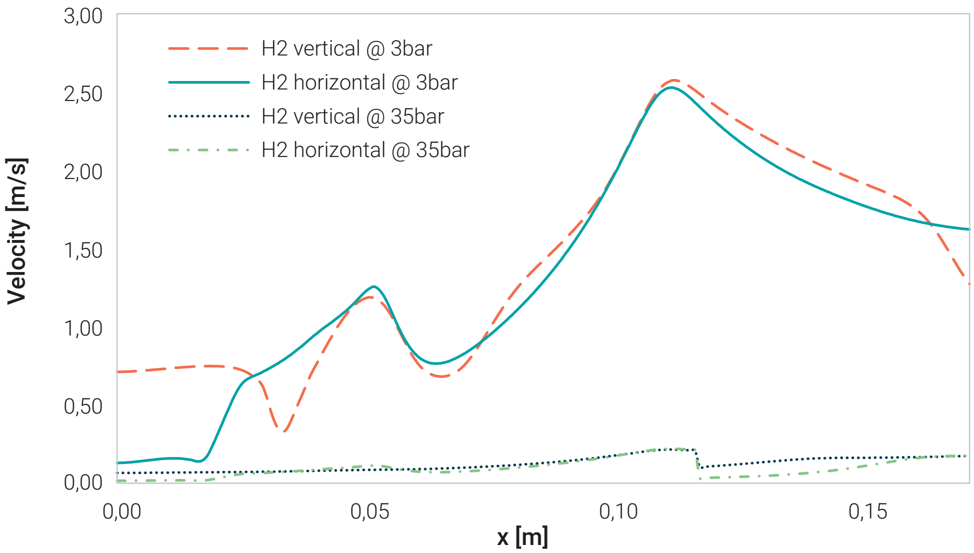

Fig. 16. Velocity Profile for the Evaluated Configurations at 3 and 35 bar.
Source: own work.

4. DISCUSSION AND CONCLUSIONS

This study numerically evaluated the impact of pressure and supply configuration on mixing efficiency using the Venturi effect for CO_2/H_2 and CH_4/H_2 mixtures in a power-to-gas conversion process. A static mixer with gas supply through a set of "T"-shaped tubes was employed. Navier-Stokes equations and conservation equations for energy and species were used to simulate the mixing process numerically. ANSYS Fluent 19.2 software was applied, utilizing finite volume discretization schemes and the standard k-ε turbulence model. The following conclusions were drawn:

- The impact of flow inlet configurations and pressure on mixing performance was investigated. It was found that the way gases are introduced into the mixer is crucial for achieving uniform distribution of gases and maximizing their interaction.
- For CO_2/H_2 mixtures, two pressures were studied: 1 bar and 4 bar. Pressure was found to affect concentration uniformity in the mixture, with 1 bar being more favorable for achieving higher uniformity. However, the proposed mixer configuration was not recommended as it did not guarantee mixing homogeneity.

- For CH_4/H_2 mixtures, two pressures were investigated: 3 bar and 35 bar. It was observed that higher pressure leads to lower concentration uniformity in the mixture. This is due to the decrease in the diffusion coefficient with increasing pressure, as predicted by the theory of transport phenomena. Therefore, the proposed mixer configuration is only recommended for pressures lower than or equal to 3 bar.
- Mixing efficiency was evaluated using the factor Z and the coefficient of variation (CoV). The use of the mixer significantly improved concentration uniformity for most cases studied, except for CH_4/H_2 at 35 bar. An average decrease of 80% in CoV was observed when comparing configurations without a mixer to configurations with a mixer for CO_2/H_2 mixtures.
- For CH_4/H_2 mixtures, there was an average 60% decrease in CoV for a pressure of 3 bar, while for a pressure of 35 bar, CoV values were very high (increasing by an average of 56%). Thus, the proposed configuration is not recommended for the latter case.
- Pressure drop generated by the mixer was negligible for all evaluated configurations, indicating good energy performance of the mixer.
- The most suitable configuration for CO_2/H_2 mixing was determined to be the horizontal introduction of H_2 for the evaluated pressures. For CH_4/H_2 mixtures, vertical H_2 supply yielded better mixing performance.

In summary, this numerical study provided insights into the impact of pressure and supply configuration on mixing efficiency using the Venturi effect for CO_2/H_2 and CH_4/H_2 mixtures in a power-to-gas process. The obtained results can be valuable for the design and optimization of mixing systems in such processes.

ACKNOWLEDGMENTS

The authors gratefully acknowledge the financial support provided by the Colombia Scientific Program within the framework of the call Ecosistema Científico (Contract No. FP44842- 218-2018). The authors also acknowledge Universidad de Antioquia-UdeA for the valuable economic contribution toward the development of this research through the “Sostenibilidad” program.

REFERENCES

[1] P. Igeland *et al*, “The energy transition: The behavior of renewable energy stock during the times of energy security uncertainty,” *Renewable Energy,* vol. 221, pp. 119746, 2024.

[2] B. Elie *et al*, “Gold and crude oil as safe-haven assets for clean energy stock indices: Blended copulas approach,” *Energy,* vol. 178, pp. 544-553, 2019.

[3] Z. Liu *et al*, “Renewable energy utilizing and fluctuation stabilizing using optimal dynamic grid connection factor strategy and artificial intelligence-based solution method,” *Renewable Energy,* vol. 219, pp. 119379, 2023.

[4] Q. Hassan *et al*, “A review of hybrid renewable energy systems: Solar and wind-powered solutions: Challenges, opportunities, and policy implications,” *Results in Engineering,* pp. 101621, 2023.

[5] R. Qiu *et al*, “Green hydrogen-based energy storage service via power-to-gas technologies integrated with multi-energy microgrid,” *Appl. Energy,* vol. 350, pp. 121716, 2023.

[6] D. Lanni *et al*, “Biomethane production through the power to gas concept: A strategy for increasing the renewable sources exploitation and promoting the green energy transition,” *Energy Conversion and Management,* vol. 293, pp. 117538, 2023.

[7] M. Lehner *et al*, “Storage options for renewable energy,” *Power-to-Gas: Technology and Business Models,* pp. 1-6, 2014.

[8] M. Thema, F. Bauer and M. Sterner, “Power-to-Gas: Electrolysis and methanation status review,” *Renewable and Sustainable Energy Reviews,* vol. 112, pp. 775-787, 2019. DOI: https://doi.org/10.1016/j.rser.2019.06.030.

[9] M. Ozturk and I. Dincer, “A comprehensive review on power-to-gas with hydrogen options for cleaner applications,” *Int J Hydrogen Energy,* vol. 46, *(62),* pp. 31511-31522, 2021. DOI: https://doi.org/10.1016/j.ijhydene.2021.07.066.

[10] M. Götz *et al*, “Renewable Power-to-Gas: A technological and economic review,” *Renewable Energy,* vol. 85, pp. 1371-1390, 2016. DOI: https://doi.org/10.1016/j.renene.2015.07.066.

[11] M. Lehner *et al*, *Power-to-Gas: Technology and Business Models.* Springer, 2014.

[12] A. Okunlola, M. Davis and A. Kumar, “The development of an assessment framework to determine the technical hydrogen production potential from wind and solar energy,” *Renewable and Sustainable Energy Reviews,* vol. 166, pp. 112610, 2022. DOI: https://doi.org/10.1016/j.rser.2022.112610.

[13] O. Tang, J. Rehme and P. Cerin, “Levelized cost of hydrogen for refueling stations with solar PV and wind in Sweden: On-grid or off-grid?” *Energy,* vol. 241, pp. 122906, 2022. DOI: https://doi.org/10.1016/j.energy.2021.122906.

[14] Y. Patcharavorachot *et al*, “Comparative energy, economic, and environmental analyses of power-to-gas systems integrating SOECs in steam-electrolysis and co-electrolysis and methanation,” *Thermal Science and Engineering Progress,* vol. 42, pp. 101873, 2023. Available: https://www-sciencedirect-com.udea.lookproxy.com/science/article/pii/S2451904923002263. DOI: https://doi.org/10.1016/j.tsep.2023.101873.

[15] R. M. Molano-Pulido, F. M. Cabrera, y F. E. Vargas-Silva, “Electronic ACPM meter in gallons, for the electric generator tank of the ESUFA radar”, Vis. Electron., vol. 16, no. 2, 2022. Available: https://revistas.udistrital.edu.co/index.php/visele/article/view/20694 DOI: 10.14483/22484728.20694.

[16] P. Straka, “A comprehensive study of Power-to-Gas technology: Technical implementations overview, economic assessments, methanation plant as auxiliary operation of lignite-fired power station,” *J. Clean. Prod.,* vol. 311, pp. 127642, 2021. Available: https://www-sciencedirect-com.udea.lookproxy.com/science/article/pii/S0959652621018606. DOI: 10.1016/j.jclepro.2021.127642.

[17] J. Fąfara and N. Modliński, “Numerical study of internal flue gas recirculation system applied to methane-hydrogen powered gas microturbine combustor.” *Combustion Engines (2300-9896),* vol. 192*(1),* pp. 63–77, 2023. DOI: https://doi.org/10.19206/CE-152236.

[18] K. K. Botros, M. Shariati and S. Sandhawalia, “Performance of five different natural gas and hydrogen blending mixer designs via CFD,” in *International Pipeline Conference,* vol. V001T08A005, pp. 1-14, 2022.

[19] T. Wang *et al*, “A numerical study on the transient injection characteristics of gas fuel injection devices for direct-injection engines,” in *Actuators, Vol. 12,* Page 102, 12 (3), 2023. DOI: https://doi.org/10.3390/act12030102.

[20] M. R. Dahake and S. E. Patil, “Experimental Study on CNG Engine with Different Ventury Configuration,” *Materials Today: Proceedings,* vol. 55, pp. 388-393, 2022. . DOI: https://doi.org/10.1016/j.matpr.2021.08.357.

[21] Q. Liu *et al*, "Analysis of the static mixer effect on natural gas mixing process in a pipeline," *Flow Meas. Instrum.,* vol. 85, pp. 102146, 2022. Available: https://www-sciencedirect-com.udea.lookproxy.com/science/article/pii/S0955598622000267. DOI: 10.1016/j.flowmeasinst.2022.102146.

[22] D. Hu *et al*, "Design and numerical simulation of a gas mixer," *Mapan,* vol. 30, pp. 203-209, 2015. DOI: https://doi.org/10.1007/s12647-015-0135-3.

[23] M. M. Haddadi *et al*, "Comparative analysis of different static mixers performance by CFD technique: An innovative mixer," *Chin. J. Chem. Eng.,* vol. 28, *(3),* pp. 672-684, 2020. DOI: https://doi.org/10.1016/j.cjche.2019.09.004.

[24] E. Fourcade *et al*, "CFD calculation of laminar striation thinning in static mixer reactors," *Chemical Engineering Science,* vol. 56, *(23),* pp. 6729-6741, 2001.

[25] J. N. Armor, "Overcoming equilibrium limitations in chemical processes," *Applied Catalysis A: General,* vol. 222, *(1-2),* pp. 91-99, 2001.

[26] C. Mejía-Botero *et al*, "Effect of preheat temperature, pressure, and residence time on methanation performance," *Energy,* vol. 269, pp. 126693, 2023. Available: https://www-sciencedirect-com.udea.lookproxy.com/science/article/pii/S0360544223000877. DOI: 10.1016/j.energy.2023.126693.

[27] G. Pluvinage, J. Capelle and M. H. Meliani, "Pipe networks transporting hydrogen pure or blended with natural gas, design and maintenance," *Eng. Failure Anal.,* vol. 106, pp. 104164, 2019.

[28] M. W. Melaina, O. Antonia and M. Penev, "Blending hydrogen into natural gas pipeline networks: a review of key issues," 2013. DOI: https://doi.org/10.2172/1068610.

[29] H. De Vries, O. Florisson and G. C. Tiekstra, "Safe Operation of Natural Gas Appliances Fuelled with Hydrogen & Natural Gas Mixtures (Progress Obtained in the Naturalhy-Project)," 2007. Available: https://h2tools.org/file/7451/download?token=4ZNOefdX.

[30] Enapter (2021). *AEM technology. Enapter handbook*. Available: https://handbook.enapter.com/electrolyser/el40/downloads/ELE40-MAN-000EN-REV05.pdf.

[31] Pedro Souza de Oliveira, João *et al*, "Coupling a neural network technique with CFD simulations for predicting 2-D atmospheric dispersion analyzing wind and composition effects," *J Loss Prev Process Ind,* vol. 80, pp. 104930, 2022. Available: https://www-sciencedirect-com.udea.lookproxy.com/science/article/pii/S0950423022002066. DOI:10.1016/j.jlp.2022.104930.

[32] Y. Zhang, M. Zhang and H. Zhou, “Mixing performance of preheated flue gas entering selective catalytic reactor under low loads,” *Appl. Therm. Eng.,* vol. 224, pp. 120049, 2023.

[33] M. Zhou *et al*, “Numerical investigation of turbulent reactive mixing in a novel coaxial jet static mixer,” *Chemical Engineering and Processing: Process Intensification,* vol. 122, pp. 190-203, 2017.

[34] Ansys (2018). *Ansys 19.2 Delivers Faster Problem-Solving Capabilities Across the Entire Portfolio.* Available: https://www.ansys.com/news-center/press-releases/09-18-18-ansys-19-2-delivers-faster-problem-solving-capabilities-across-entire-portfolio.

[35] S. V. Patankar, “Numerical heat transfer and fluid flow, Hemisphere Publ,” *Corp., New York,* vol. 58, pp. 288, 1980.

[36] C. Habchi *et al*, “Mixing performance in split-and-recombine milli-static mixers—A numerical analysis,” *Chem. Eng. Res. Design,* vol. 142, pp. 298-306, 2019. . DOI: https://doi.org/10.1016/j.cherd.2018.12.010.

[37] M. Y. L. Pérez *et al*, “Análisis de modelaciones de canal abierto con reducción en OpenFOAM,” *Ingeniería Solidaria,* vol. 19, *(2),* pp. 1-21, 2023.

[38] A. W. Nienow, M. F. EDWARDS and N. Harnby, *Mixing in the Process Industries.* Elsevier Science, 1997.

[39] L. J. Dietsche and A. C. Neubauer, “Computational fluid dynamics model of viscous droplet breakup,” *Chemical Engineering Science,* vol. 64, *(22),* pp. 4543-4552, 2009. Available: https://doi.org/10.1016/j.ces.2009.06.046.

[40] C. K. Law, *Combustion Physics.* Cambridge University Press, 2010.